Astron. Nachr. / AN **999**, No. 88, 789 – 796 (2006) / **DOI** ***please set DOI!***

New Radial Velocities for 30 Candidate Runaway Stars and a Possible Binary Supernova Origin for HIP 9470 and PSR J0152−1637

N. Tetzlaff[1,⋆], **G. Torres**[2], **A. Bieryla**[2], and **R. Neuhäuser**[1]

[1] Astrophysikalisches Institut und Universitäts-Sternwarte Jena, Schillergässchen 2-3, 07745 Jena, Germany
[2] Harvard-Smithsonian Center for Astrophysics, 60 Garden St., Cambridge, MA 02138, USA

Received ., accepted .
Published online .

Key words (stars:) binaries: spectroscopic, stars: kinematics, (stars:) pulsars: individual: PSR J0152−1637

We report new radial velocity measurements for 30 candidate runaway stars. We revise their age estimates and compute their past trajectories in the Galaxy in order to determine their birthplaces. We find that seven of the stars could be younger than ∼100 Myr, and for five of them we identify multiple young clusters and associations in which they may have formed. For the youngest star in the sample, HIP 9470, we suggest a possible ejection scenario in a supernova event, and also that it may be associated with the young pulsar PSR J0152−1637. Our spectroscopic observations reveal seven of the stars in the sample of 30 to be previously unknown spectroscopic binaries. Orbital solutions for four of them are reported here as well.

© 2006 WILEY-VCH Verlag GmbH & Co. KGaA, Weinheim

arXiv:1409.0822v1 [astro-ph.SR] 2 Sep 2014

1 Introduction

The first studies of high velocity stars were carried out by A. Blaauw and collaborators as early as the 1950's (Blaauw 1952; Blaauw & Morgan 1954). Blaauw (1961) examined a number of O- and B-type stars and found that many of them had space velocities in excess of 40 km/s. He referred to these objects as "runaway stars", a term that has been used ever since.

Runaway stars are mainly produced via two mechanisms. The binary supernova scenario (BSS) was first proposed by Blaauw (1961). It is also related to the formation of high velocity neutron stars. The runaway and the neutron star are the products of a supernova within a binary system. The velocity of the former secondary (the runaway star) may be as large as its original orbital velocity (Tauris & Takens 1998). The kinematic age of a BSS runaway star is smaller than the age of its parent association since the primary star needed some time to evolve and experience a supernova. In the alternate dynamical ejection scenario (DES) that was suggested by Poveda et al. (1967), stars are ejected from young, dense clusters via gravitational interactions between the cluster members. The (kinematic) age of a DES runaway star should be comparable to the age of its parent association since gravitational interactions are most efficient soon after formation.

To investigate the frequency of runaway stars among all stars in the Galaxy, Stone (1991) proposed fitting the velocity distribution with two Maxwellians, one representing normal Population I stars, the second one explaining the group of runaway stars. While many studies aiming at identifying runaway stars were based on space velocities (e. g. Blaauw 1961), tangential velocities (e. g. Moffat et al. 1998) or radial velocities (e. g. Cruz-González et al. 1974) alone, we recently constructed a unified catalogue of young runaway stars by evaluating all these criteria as well as the direction of motion compared to its neighbourhood (Tetzlaff et al. 2011b).

Although absolute 3D velocities are not essential to identify runaway stars, they are necessary for constructing stellar orbits. Past stellar trajectories can be used to identify the parent association or cluster of a star and its runaway origin. Some runaway stars have been proposed as former companion candidates to the progenitors of neutron stars (Hoogerwerf et al. 2001; Tetzlaff 2013; Tetzlaff et al. 2011a, 2012). Such an association may explain the spectral properties of a runaway star, such as a high Helium abundance or high rotational velocity or even enhanced α element abundances as supernova debris (Blaauw 1993; Przybilla et al. 2008).

In this paper we investigate the nature of 30 of the candidate runaway stars proposed by Tetzlaff et al. (2011b). Kinematic information for these objects was previously incomplete because of missing radial velocities (v_r). Here we present multiple measurements of v_r for these stars, and in addition we revise their age estimates from the work mentioned above. With this information we construct and trace back the Galactic orbits for the young stars in the sample to investigate their origin and possible connection with young clusters and neutron stars. Seven of the targets are revealed to be spectroscopic binaries, and orbits for four of them are reported here.

⋆ Corresponding author: e-mail: nina@astro.uni-jena.de

© 2006 WILEY-VCH Verlag GmbH & Co. KGaA, Weinheim

2 Spectroscopy and Radial Velocities

Spectroscopic observations of our 30 targets were gathered using the Tillinghast Reflector Echelle Spectrograph (TRES, Fűrész 2008) on the 1.5 m Tillinghast reflector at the F. L. Whipple Observatory (Mount Hopkins, Arizona, USA), from 2011 April to 2013 October. Individual stars were observed for periods ranging from ∼1 yr to a little over 2 yr. The spectra cover the wavelength range ∼3900–8900 Å, and were taken with a typical resolving power of $R \sim 44{,}000$ with the medium fiber of the instrument. The signal-to-noise ratios for the individual exposures range between 23 and 230 per resolution element of $6.8\,\mathrm{km/s}$, and refer to the region of the Mg I b triplet (∼5200 Å). All spectra were reduced and extracted using standard procedures as described by Buchhave (2010) and Buchhave et al. (2010).

Radial velocities were obtained by cross-correlation against a synthetic template taken from a large library computed by John Laird, based on model atmospheres by R. L. Kurucz and a line list developed by Jon Morse (see Buchhave et al. 2012). These templates cover a 300 Å window centred at 5200 Å, which generally contains most of the velocity information, and have a spacing of 250 K in temperature ($T_{\rm eff}$), 0.5 dex in surface gravity ($\log g$) and metallicity ([Fe/H]), and a variable step in the projected rotational velocity ($v \sin i$). The optimum template for each star was determined by cross-correlating all observations against the entire library of templates, and choosing the one giving the highest correlation coefficient averaged over all exposures (Torres et al. 2002). The best-matched template provides an estimate of the stellar parameters, although their accuracy is limited by degeneracies that are present among $T_{\rm eff}$, $\log g$, and [Fe/H]. The template parameters that affect the velocities the most are $T_{\rm eff}$ and $v \sin i$. To suppress correlations, in a second iteration we held the metallicity fixed at the solar value and $\log g$ at values determined with the help of stellar evolution models as described in the next section. We then redetermined $T_{\rm eff}$ and $v \sin i$, and recomputed the velocities.

The zero point of our velocity system was monitored by observing standard stars each night with the same instrumental setup. Individual heliocentric velocities for each of our candidate runaway stars are reported in Table 1 (the complete table is available as supplementary material). In Table 2 we report the average v_r of each star, along with the template parameters and other pertinent information.

2.1 Binary systems

Seven of our targets have variable radial velocity and are spectroscopic binaries. For four of them we gathered sufficient observations to solve for the orbital elements, which are presented in Table 3. In two cases (HIP 101219 and HIP 113787) the eccentricities turned out not to be significant; the solutions presented for those stars assume the orbits to be circular. The velocities listed for these binaries in Table 2 correspond to the systemic velocity. The other three variables show only long-term drifts over the time span of our observations, and their orbital periods are likely to be several years. Therefore, the mean velocities listed for these stars in Table 2 do not necessarily represent the true centre-of-mass velocity. The orbital solutions are shown graphically in Fig. 1, along with the time histories of the three objects with long-term trends.

Table 1 Individual radial velocities (with 1σ errors) for each of the 30 stars in our sample. Only the measurements for HIP 8414 are shown here. The full table is available as Supporting Information with this article. Here only the measurements for HIP 8414 are shown (this star happens to have variable radial velocity; see Fig. 1).

HIP	HJD-2,400,000	v_r
8414	55757.9805	−29.88±0.60
8414	55824.9922	−2.13±0.57
8414	55840.9297	−21.22±0.53
8414	55884.7539	−34.63±0.78
8414	55905.6914	−34.76±0.64
8414	55960.6094	8.42±0.60
8414	55983.5820	−17.31±0.62
8414	56231.7500	2.51±0.47
8414	56253.6953	−34.13±0.56
8414	56316.5703	−33.71±0.57
8414	56496.9492	−12.87±0.64
8414	56549.8203	−32.10±0.69
8414	56550.8438	−8.26±0.58
8414	56559.9063	−28.48±0.59
8414	56574.9102	14.45±0.76
8414	56592.7305	−16.79±0.59

Three of the four stars with spectroscopic orbits (HIP 9470, HIP 101219, and HIP 113787), as well as the three with long-term trends, are slowly rotating G or K giants (see below) and their orbital periods are long. The other binary with a spectroscopic orbit (HIP 8414) has a short period, and the rapidly rotating primary star is an F dwarf. Its measured rotation ($v \sin i = 42\,\mathrm{km/s}$) is consistent with the star being pseudo-synchronized with motion in the slightly eccentric orbit (Hut 1981).

3 Past Trajectories

In order to construct the past orbits of our sample stars, stellar ages are required. In our previous study (Tetzlaff et al. 2011b) we already reported age estimates by comparison with evolutionary models in order to focus on the younger runaway candidates, as past orbits become too uncertain for older objects. The temperatures of the stars used to place them on the H-R diagram were based on published spectral types, and the conversion table of Schmidt-Kaler (1982). However, because of variations in chemical composition the zero-age main sequence (ZAMS) has some spread at a given effective temperature, which could not be resolved for the objects in our earlier study because we lacked estimates of the metallicity. To be conservative and not miss potentially

© 2006 WILEY-VCH Verlag GmbH & Co. KGaA, Weinheim

Table 2 Mean radial velocities v_r of 30 stars (column 5). The errors represent 1σ uncertainties.
Columns 2 to 4 list the stellar properties: visual magnitude **V**, effective temperature ($T_{\rm eff}$ in K), surface gravity in standard (cgs) units ($\log g$) and projected rotational velocity ($v \sin i$ in km/s). In columns 6 and 7 we give the number of spectra (N) and the time (in days) spanned by the spectroscopic observations for each star, respectively. The last column contains information on multiplicity (SB1 for single-lined spectroscopic binary).

HIP	V	$T_{\rm eff}$	$\log g$	$v \sin i$	v_r	N	span	Notes
8414	8.50	6600±100	4.23	42±4	−13.06±0.22	16	835	SB1, $P = 1.74$ d, additional visual companion at 1.7" (Lampens et al. 2007), implying a triple system
9470	6.54	5000±100	1.54	8±2	−11.91±0.10	12	749	SB1, $P = 558$ d
10784	6.88	4600±100	1.92	4±1	+34.85±0.05	7	400	
18549	8.51	8000±250	4.16	151±15	+3.97±1.35	6	351	
27802	10.39	4700±100	4.19	2±1	+14.75±0.06	11	436	
39228	10.06	5600±100	4.56	1±1	−4.51±0.05	8	396	Secondary in double system with HIP 39226
42331	7.60	4050±100	1.27	4±1	+3.83±0.37	17	774	Long-term drift
43043	7.99	7400±100	4.20	56±4	+25.11±0.09	9	396	
49820	10.36	7150±100	4.29	51±4	+9.12±0.13	13	632	
60065	10.36	7350±150	4.32	152±15	−15.58±0.79	9	388	
70995	10.60	5900±100	4.56	2±1	−3.39±0.07	9	388	
82163	7.91	4200±100	1.54	4±1	−64.77±1.12	16	773	Long-term drift
82304	7.35	3850±100	1.16	6±1	−27.41±0.04	9	416	
83627	8.46	7700±100	4.21	11±2	−20.56±0.11	10	347	
84385	7.12	3650±100	1.03	7±2	+15.00±0.17	19	768	
85271	7.74	3800±100	1.31	6±1	−53.01±0.06	14	768	
91545	8.32	7350±150	4.25	159±15	−43.99±0.89	7	360	
96045	7.61	4100±100	1.37	5±1	−52.12±0.05	8	530	
98019	8.16	4500±100	1.79	6±1	−4.22±0.03	7	381	
98443	6.98	4050±100	1.43	6±1	−42.54±1.37	15	731	Long-term drift, primary in triple system (Anosova et al. 1987)
101219	7.50	3700±100	0.98	4±1	−5.00±0.06	15	895	SB1, $P = 483$ d
101320	7.68	4900±100	1.95	5±1	−18.74±0.01	7	377	
102000	9.14	9150±100	4.28	80±4	+2.76±0.47	14	751	
103533	8.61	5500±150	3.02	154±20	+26.67±4.03	12	751	Secondary in double system with HIP 103537
104581	10.09	5300±100	4.61	2±1	−21.54±0.06	6	514	Primary in double system with K3 type star
104608	11.01	7250±100	4.17	50±4	+3.23±0.25	6	509	
106291	9.25	7250±100	4.32	20±3	+5.21±0.03	6	514	
111607	8.06	4350±100	1.76	3±1	+21.64±0.05	7	718	
113787	6.56	4800±100	2.04	5±1	+4.40±0.02	13	589	SB1, $P = 467$ d
117998	8.30	7450±100	4.23	94±5	+12.25±0.50	8	414	

Note: The $\log g$ values were estimated from stellar evolution models based on preliminary temperature estimates, and were held fixed (along with an assumed solar metallicity) to infer the final temperatures reported here (see text). The uncertainties reported for the velocities are the standard error of the mean.

young objects, late-type stars that were found to fall below the solar-metallicity ZAMS in the H-R diagram were shifted upwards in luminosity onto the model ZAMS. This most likely resulted in underestimated ages for those stars.

For the 30 stars in the present sample we now have available the spectroscopic temperatures determined by cross-correlation. To compute stellar luminosities L, we determined the distances from their HIPPARCOS parallaxes (van Leeuwen 2007) using equation 2.11 of Francis (2013). This prescription yields results that are on average less affected by the bias towards larger distances arising from the parallax errors and the reciprocal relation between distance and parallax[1]. Two of the stars, HIP 39228 and HIP 103533, are the secondaries in visual pairs, and their nominal parallaxes have very large uncertainties caused by the presence of the brighter primaries, and may be biased for the same reason. For those stars we adopted the catalogue values listed for the primaries. We further used the V magnitudes as re-

[1] The distance formula by Francis (2013) is strictly valid for parallax errors below 20 per cent. Although many of the stars in our sample exceed this limit, we have chosen to use the same expression because numerical simulations of a sample of 20,000 stars show that the resulting distances are still closer to the true distances than the nominal values. This procedure is also preferable to other approaches such as that of (Smith & Eichhorn 1996), as shown by the same simulations.

© 2006 WILEY-VCH Verlag GmbH & Co. KGaA, Weinheim

Table 3 Orbital solutions for four binary stars.
P – orbital period, γ – systemic velocity, K – velocity semi-amplitude of the primary, e – eccentricity, ω – longitude of periastron, T – time of periastron passage for systems with eccentric orbits or time of maximum velocity for systems with circular orbits, $a_1 \sin i$ – projected semimajor axis of the primary star, $f\,(M)$ – mass function, $M_2 \sin i$ – minimum mass of secondary, σ – root-mean-square residual from the fit.

Element	HIP 8414	HIP 9470	HIP 101219	HIP 113787
P [d]	1.740469 ± 0.000020	556.5 ± 1.5	545 ± 23	467.12 ± 0.94
γ [km/s]	-13.06 ± 0.22	-11.912 ± 0.099	-4.995 ± 0.055	4.402 ± 0.016
K [km/s]	24.77 ± 0.43	10.174 ± 0.088	0.56 ± 0.08	3.932 ± 0.022
e	0.165 ± 0.018	0.3568 ± 0.0064	0 (fixed)	0 (fixed)
ω [deg]	326.0 ± 3.7	159.06 ± 0.83	...	...
T [HJD]	2456205.734 ± 0.017	2456194.6 ± 2.4	2456178 ± 13	2455985.20 ± 0.44
$a_1 \sin i$ [Gm]	0.5847 ± 0.0090	72.73 ± 0.74	4.17 ± 0.64	25.26 ± 0.13
$f\,(M)$ [$M_\odot$]	$(2.63 \pm 0.12) \cdot 10^{-3}$	$(4.95 \pm 0.15) \cdot 10^{-2}$	$(9.7 \pm 4.1) \cdot 10^{-6}$	$(2.943 \pm 0.048) \cdot 10^{-3}$
$M_2 \sin i$ [$(M_1 + M_2)^{2/3}$ [$M_\odot$]]	0.1380 ± 0.0021	0.3672 ± 0.0036	0.0213 ± 0.0030	0.14330 ± 0.00078
number of observations	16	12	15	13
span of observations [d]	834.8	748.9	894.6	588.6
σ [km/s]	0.81	0.06	0.20	0.05

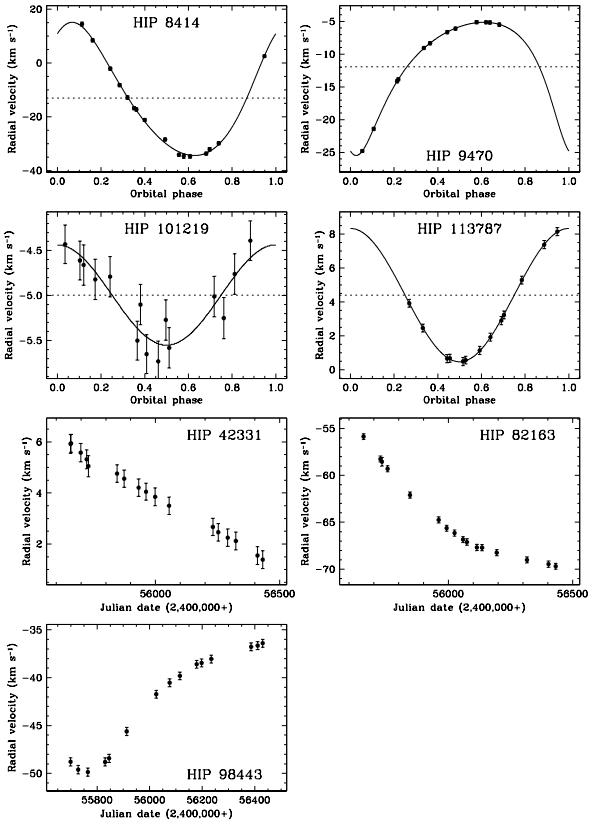

Fig. 1 Orbital solutions for four binary stars and time histories of three objects with long-term trends.

ported in the Tycho-2 catalog (Høg et al. 2000) converted to the Johnson system, and an estimate of the extinction based on the $B - V$ indices (converted from the Tycho-2 measurements) and standard colours for main sequence and giant stars (see Tetzlaff et al. 2011b and Tetzlaff 2013). Approximately half of our stars are found to be evolved. Ages and masses were inferred by comparison with several series of stellar evolution calculations (Bertelli et al. 2008, 2009; Pietrinferni et al. 2004; Schaerer et al. 1993; Schaller et al. 1992[2]), accounting for all uncertainties by utilizing a Monte Carlo method. The corresponding $\log g$ values were used to help establish the spectroscopic temperatures, as described earlier. However, the limitation due to the unknown metallicities remains, as we cannot determine [Fe/H] reliably from our spectroscopic material due to the strong correlations with $T_{\rm eff}$ and $\log g$ mentioned in section 2. Therefore, we do not determine ages and masses for nine stars that fall below the solar-metallicity ZAMS (Fig. 2); those objects are likely old in any case, which prevents a reliable determination of their Galactic orbits. The masses and ages determined for the remaining 21 stars are listed in Table 4. We note that among these 21 stars there are 14 stars that are located in the upper right part of the HR diagram and, hence, are possibly evolve stars. Some of them are probably already old.

With knowledge of the distance and kinematics (proper motions[3] and our new v_r measurements), we used the fourth-order Runge-Kutta algorithm implemented in MATLAB© to calculate the past stellar trajectories. We adopted an axisymmetric Galactic potential that contains a Miyamoto-Nagai potential for the disk (Miyamoto & Nagai 1975), a Hernquist potential for the bulge and the inner halo (Hernquist 1990) and a logarithmic potential for the dark halo, see Harding et al. (2001). For seven stars that could clearly be younger than 100 Myr (marked with an asterisk in Table 4), we compared the past flight paths

[2] Isochrones from Schaller et al. (1992) and Schaerer et al. (1993) were obtained from the database http://webast.ast.obs-mip.fr/equipe/stellar/ (Lejeune & Schaerer 2001). For Pietrinferni et al. (2004), see also the BaSTI web tools (http://albione.oa-teramo.inaf.it/).

[3] We consistently use proper motions and parallaxes from HIPPARCOS (van Leeuwen 2007).

© 2006 WILEY-VCH Verlag GmbH & Co. KGaA, Weinheim

Table 4 Evolutionary ages $\tau_\star$ and masses $m_\star$ for 21 stars. The errors include the uncertainty on the parallax, V magnitude, $B-V$ colour, $T_{\rm eff}$, the spread between different evolutionary models as well as a lower metallicity of $[{\rm Fe/H}] = -0.4$. The nominal values for mass and age represent the respective median for solar metallicity. Stars that are marked with an asterisk (*) could clearly be younger than $100\,{\rm Myr}$, the other stars are most probably a few hundred up to a few thousand Myr old. Note that we did not consider HIP 82304, HIP 83627, HIP 111607 and HIP 117998 young stars. For the first three of these stars, median ages of $\sim 600-800\,{\rm Myr}$ suggest that the stars are not young and the lower age bound does not clearly fall below our $100\,{\rm Myr}$ limit. For HIP 117998 the lower age bound is relatively small suggesting that the star is older than $100\,{\rm Myr}$.

HIP	$\tau_\star$ [Myr]	$m_\star$ [$M_\odot$]
8414	2000^{+2000}_{-1300}	$1.3^{+0.1}_{-0.3}$
9470*	65^{+91}_{-20}	$6.0^{+2.2}_{-2.2}$
10784*	168^{+600}_{-70}	$3.9^{+1.9}_{-1.9}$
27802	~ 14000[a]	$0.6^{+0.3}_{-0.1}$
39228	~ 10000[a]	$1.0^{+0.1}_{-0.3}$
42331	1000^{+5000}_{-820}	$3.0^{+5.9}_{-2.6}$
43043	1000^{+2000}_{-540}	$1.5^{+0.1}_{-0.2}$
82163	570^{+3900}_{-450}	$3.0^{+4.6}_{-2.1}$
82304	570^{+3500}_{-430}	$1.7^{+3.8}_{-1.2}$
83627	800^{+1200}_{-700}	$1.7^{+0.1}_{-0.3}$
84385*	400^{+5500}_{-350}	$3.9^{+1.6}_{-3.4}$
85271	$1000^{+\ldots}_{-800}$ [b]	$0.9^{+2.3}_{-0.5}$
91545	1000^{+2000}_{-600}	$1.6^{+0.1}_{-0.3}$
96045	550^{+6500}_{-350}	$3.5^{+6.5}_{-2.7}$
98019*	150^{+3000}_{-50}	$4.3^{+1.6}_{-3.8}$
98443*	118^{+5100}_{-50}	$4.6^{+1.6}_{-4.1}$
101219	6600^{+7400}_{-6400}	$2.8^{+5.6}_{-2.5}$
101320*	120^{+14000}_{-70}	$2.9^{+4.1}_{-2.2}$
111607	570^{+4500}_{-470}	$2.0^{+4.3}_{-1.4}$
113787*	168^{+178}_{-79}	$4.3^{+0.8}_{-1.5}$
117998	200^{+2800}_{-90}	$1.5^{+0.1}_{-0.1}$

[a] These stars are too old for precise age estimate with our methods.

[b] The upper age limit of HIP 85271 cannot be constrained by our methods.

with those of young associations (see Tetzlaff 2013; Tetzlaff et al. 2010, 2012) and 42 stellar clusters with ages between 40 and $150\,{\rm Myr}$ from Bukowiecki et al. (2012) for which 3D kinematic data are available. The kinematic properties of the clusters where obtained from Dias et al. (2006), Kharchenko et al. (2005), Wu et al. (2009) and Vande Putte et al. (2010), or derived as the mean values of members listed in the WEBDA database[4] (Mermilliod & Paunzen 2003). Due to the positional uncertainties of the associations/clusters that increase with time because of their velocity dispersion, we calculate the past flight paths only up to $150\,{\rm Myr}$. For the same reason, we did not account for association/cluster expansion or evaporation effects because the positional uncertainties dominate.

[4] http://www.univie.ac.at/webda/

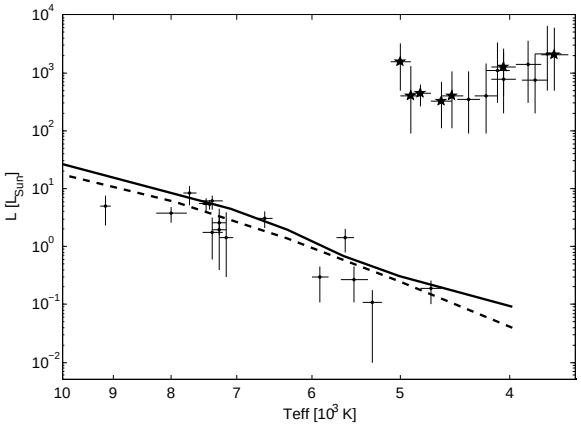

Fig. 2 The 30 stars in our sample shown on the H-R diagram. Objects indicated by a star are possibly young (up to $\sim 100\,{\rm Myr}$) stars. The solid and dashed lines indicate the mean model ZAMS for solar metallicity and $[{\rm Fe/H}] = -0.4$, respectively.

For five stars, we found multiple possible birth clusters (for flight times below $150\,{\rm Myr}$) that we list in Table 5 along with the flight time and the cluster age. In these cases, taking the positional and kinematic uncertainties into account, the runaway star was probably inside the boundaries of the association/cluster within the past $150\,{\rm Myr}$.

The flight time to reach the Galactic plane is smaller than the stellar ages for all cases as half the period of the vertical oscillation is smaller than the stellar age. Therefore, we cannot make statements about whether any of these stars were born in the Galactic plane.

We also calculated the past trajectories of young neutron stars in order to find possible encounters with runaway stars. We note, however, that only about 35 per cent of former runaway star/neutron star pairs can be recovered due to the large uncertainties on the observables (Tetzlaff 2013). Owing to the unknown radial velocity of neutron stars, their flight paths can only be traced back up to a maximum of a few Myr (we use $5\,{\rm Myr}$, e. g. Tetzlaff 2013; Tetzlaff et al. 2011a, 2010). This also sets a limit on the maximum age of the runaway star. Assuming that the neutron star is $5\,{\rm Myr}$ old and that the mass of its progenitor was the minimum mass required for a supernova progenitor ($\sim$B3, implying a lifetime of $\sim 30-40\,{\rm Myr}$), the only suitable runaway star in our sample is HIP 9470 (allowing for some Myr uncertainty on the progenitor lifetime and the stellar age).

To search for a neutron star that may potentially be related to HIP 9470, we apply a Monte Carlo method as done

© 2006 WILEY-VCH Verlag GmbH & Co. KGaA, Weinheim

Table 6 Predicted current parameters of PSR J0358+5413 and PSR J0152−1637 and supernova position and time for a possible past encounter with HIP 9470.
Neutron star parameters: heliocentric radial velocity v_r, distance d or parallax π, proper motion μ^*_α, μ_δ, peculiar space velocity v_{sp}; Predicted supernova position: distance of the supernova to Earth at the time of the supernova ($d_{\odot,SN}$) and as seen today ($d_{\odot,today}$), Galactic coordinates (Galactic longitude l, Galactic latitude b, J2000.0) as seen from the Earth today; Predicted time of the supernova in the past τ. For the derivation of the parameters we refer the reader to the work of Tetzlaff et al. 2010.

Present-day parameters of	PSR J0358+5413		PSR J0152−1637	
	predicted	measured[a]	predicted	measured[b]
v_r [km/s]	211^{+114}_{-38}	–	134^{+117}_{-59}	–
π [mas] or d [pc]	$0.7^{+0.1}_{-0.2}$	0.91 ± 0.16	833^{+167}_{-119}	510, 790
μ^*_α [mas/yr]	9.2 ± 0.2	9.20 ± 0.18	2.9 ± 1.1	3.1 ± 1.2
μ_δ [mas/yr]	8.3 ± 0.4	8.17 ± 0.39	-27.5 ± 2.0	-27 ± 2
v_{sp} [km/s]	266^{+101}_{-57}	–	175^{+86}_{-70}	–
Predicted supernova position and time since the explosion				
$d_{\odot,SN}$ [pc]	453^{+109}_{-52}		464^{+97}_{-82}	
$d_{\odot,today}$ [pc]	451^{+91}_{-57}		578^{+84}_{-90}	
l [°]	$149.4^{+2.4}_{-2.4}$		$149.9^{+2.1}_{-2.2}$	
b [°]	$-49.8^{+1.2}_{-1.5}$		$-49.7^{+1.1}_{-1.6}$	
τ [Myr]	~ 5		$2.1^{+0.5}_{-0.5}$	

[a] Distance from dispersion measure for two models of the Galactic electron density (Cordes & Lazio 2002; Taylor & Cordes 1993). Proper motion from Brisken et al. (2003)
[b] Chatterjee et al. (2004)

Table 5 Possible birth clusters for five young sample stars along with the flight time of the star. Ages are taken from Kharchenko et al. (2005), Dias et al. (2006), Vande Putte et al. (2010) and Bukowiecki et al. (2012).

HIP	cluster	flight time [Myr]	cluster age [Myr]
9470	NGC 103	135^{+10}_{-15}	$112 - 134$
	NGC 1444	36^{+57}_{-36}	$79 - 92$
	NGC 2353	91^{+54}_{-28}	$89 - 126$
84385	NGC 103	92^{+10}_{-9}	$112 - 134$
	NGC 436	109^{+2}_{-1}	$84 - 126$
	NGC 2353	50^{+43}_{-37}	$89 - 126$
	Pismis 16	63^{+5}_{-2}	$52 - 79$
	NGC 6694	67^{+1}_{-1}	$79 - 85$
	NGC 1513	59^{+115}_{-59}	79
	NGC 7086	98^{+7}_{-4}	$112 - 139$
98019	NGC 7086	105^{+10}_{-15}	$112 - 139$
	NGC 2353	100^{+37}_{-27}	$89 - 126$
	NGC 5617	100^{+8}_{-10}	$79 - 112$
98443	BH 92	58^{+1}_{-2}	56
	NGC 7086	150^{+4}_{-4}	$112 - 139$
113787	NGC 7788	120^{+7}_{-5}	$30 - 158$
	NGC 1778	134^{+4}_{-3}	$126 - 151$
	NGC 2186	101^{+2}_{-2}	$55 - 200$

previously by Hoogerwerf et al. (2001), Bobylev & Bajkova (2009), and by ourselves (Tetzlaff et al. 2014, 2011a, 2009, 2010, 2012, 2013), to account for all errors on the observables. Among all young nearby neutron stars[5] in the ATNF pulsar database[6] with available distance and proper motion (105 neutron stars in total, see Tetzlaff 2013), we find two candidates for a common origin with HIP 9470: PSR J0358+5413 and PSR J0152−1637. The present neutron star parameters and the position and time of the predicted supernova event are given in Table 6. The kinematic age (flight time) of PSR J0358+5413 is $\sim 5\,\mathrm{Myr}$ if HIP 9470 is its former companion. This exceeds the spin-down age by one order of magnitude ($\tau_{sd} = 564\,\mathrm{kyr}$, period P and its derivative $\dot{P}$ from Hobbs et al. 2004). Noutsos et al. (2013) determined the kinematic age as $0.5^{+0.5}_{-0.2}\,\mathrm{Myr}$ assuming that the pulsar was born in the Galactic plane which is in good agreement with τ_{sd}. Therefore, we do not consider it likely for the progenitor of PSR J0358+5413 to have been a former companion of HIP 9470. The pulsar was probably born in the Galactic plane half a million years ago.

The spin-down age of PSR J0152−1637 of $10.1\,\mathrm{Myr}$ (P and $\dot{P}$ from Hobbs et al. 2004) is a factor of five larger than our predicted kinematic age. For many neutron stars,

[5] Because of the large uncertainties on the observables of neutron stars and the unknown radial velocity, their flight paths can only be traced back up to a maximum of $\sim 5\,\mathrm{Myr}$. As the spin-down age only gives a rough estimate of the order of magnitude of the true age, neutron stars with spin-down ages up to $50\,\mathrm{Myr}$ were selected for investigation allowing for an uncertainty on the age of one order of magnitude to be conservative.

[6] Pulsar database operated by the Australia Telescope National Facility, Manchester et al. (2005), http://www.atnf.csiro.au/research/pulsar/psrcat/.

© 2006 WILEY-VCH Verlag GmbH & Co. KGaA, Weinheim

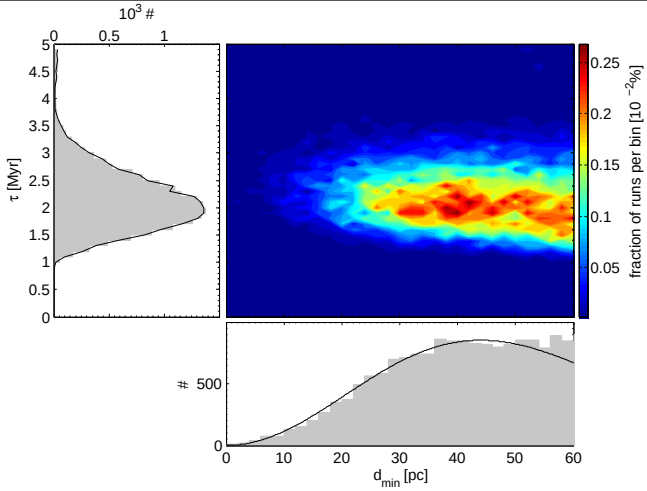

Fig. 3 Distributions of minimum separations d_{min} and corresponding flight times τ for encounters between HIP 9470 and PSR J0152−1637. The solid curve drawn in the d_{min} histogram (bottom panel) represents the theoretically expected distribution (see e. g. Tetzlaff et al. 2012) with an expectation value for the separation of zero and a standard deviation of 31.1 pc. The smallest separation between the two stars found after three million Monte Carlo runs was 1 pc. This is expected from simulated test cases (Tetzlaff 2013).

kinematic ages are smaller than τ_{sd} by a factor of a few (e. g. Hoogerwerf et al. 2001; Tetzlaff et al. 2011a, 2013). The distance of the pulsar is rather uncertain and no parallax has been measured to date. Depending on the Galactic electron density model, dispersion measured distances range from about 500 to 800 pc (Cordes & Lazio 2002; Taylor & Cordes 1993). Our predicted distance of 833^{+167}_{-119} is in reasonable agreement with these estimates.

The distribution of separations d_{min} between HIP 9470 and PSR J0152−1637 along with the flight time distribution is shown in Fig. 3. The solid line in the bottom panel represents the theoretical curve for the case that both objects met at the same position in space and is in good agreement with the d_{min} histogram (see e. g. Tetzlaff et al. 2011a, Tetzlaff 2013 and Tetzlaff et al. 2014 for similar cases).[7]

The encounter position cannot be associated with any particular stellar group that might have hosted the supernova, i. e., the predicted supernova event happened in isolation. This is possible if the neutron star progenitor itself was a runaway star. The former companion candidate HIP 9470 happens to be a binary star, as revealed by our spectroscopic monitoring. If PSR J0152−1637 and HIP 9470 were ejected during the same supernova event, this implies that the progenitor must have been at least a hierarchical triple system. This is not unlikely since stars ejected via gravitational interactions can be single, binary or triple stars (e.g. Leonard 1989). The wide orbit of the binary might be a result of the supernova explosion.

[7] The theoretical curve shows the distribution of differences between two 3D Gaussians that are centred at the same point in space (see e. g. Hoogerwerf et al. 2001; Tetzlaff et al. 2012), i. e. from the distribution we assume that the two stars were at the same spatial position about 2 Myr ago.

4 Conclusions

We have carried out high-resolution spectroscopic monitoring of 30 stars previously included in the catalogue of candidate young runaway stars of Tetzlaff et al. (2011b), for the purpose of measuring their radial velocities accurately. With this and other existing information we were able to calculate their Galactic orbits and investigate their origin in the context of runaway star scenarios. Ages for the targets were revised from previous estimates, and seven of the stars were found to be consistent with being younger than 100 Myr, and therefore still plausible as runaway stars. The remaining 23 objects are old enough that we no longer consider them to be candidate runaway stars. We computed the past orbits of the seven younger stars, and for five of them we identified several young clusters or associations with known kinematics with which they appear to have crossed paths in the recent past, suggesting this may be their place of birth. Of these five stars, the properties of HIP 9470 are consistent with it having had a recent close encounter with the neutron star PSR J0152−1637, but not simultaneously with any of the clusters. Seven of the 30 stars in the sample are found to be spectroscopic binaries, and orbital solutions for four of them are reported here.

Acknowledgements. NT and RN acknowledge partial support from DFG in the SFB/TR-7 Gravitational Wave Astronomy.
This work has made use of BaSTI web tools (http://albione.oa-teramo.inaf.it/), the database by Lejeune and Schaerer (http://webast.ast.obs-mip.fr/equipe/stellar/, Lejeune & Schaerer 2001) and the Padova database of stellar evolutionary tracks and isochrones (http://pleiadi.pd.astro.it/).

References

Anosova, Z. P., Sementsov, V. N., & Tokovinin, A. A. 1987, Soviet Ast., 31, 220
Bertelli, G., Girardi, L., Marigo, P., & Nasi, E. 2008, A&A, 484, 815
Bertelli, G., Nasi, E., Girardi, L., & Marigo, P. 2009, A&A, 508, 355
Blaauw, A. 1952, Bull. Astron. Inst. Netherlands, 11, 414
Blaauw, A. 1961, Bull. Astron. Inst. Netherlands, 15, 265
Blaauw, A. 1993, in Astronomical Society of the Pacific Conference Series, Vol. 35, Massive Stars: Their Lives in the Interstellar Medium, ed. J. P. Cassinelli & E. B. Churchwell, 207–+
Blaauw, A. & Morgan, W. W. 1954, ApJ, 119, 625
Bobylev, V. V. & Bajkova, A. T. 2009, Astronomy Letters, 35, 396
Brisken, W. F., Fruchter, A. S., Goss, W. M., Herrnstein, R. M., & Thorsett, S. E. 2003, AJ, 126, 3090
Buchhave, L. A. 2010, PhD thesis, University of Copenhagen, Denmark
Buchhave, L. A., Bakos, G. Á., Hartman, J. D., & et al. 2010, ApJ, 720, 1118

© 2006 WILEY-VCH Verlag GmbH & Co. KGaA, Weinheim

Buchhave, L. A., Latham, D. W., Johansen, A., & et al. 2012, Nature, 486, 375
Bukowiecki, Ł., Maciejewski, G., Konorski, P., & Niedzielski, A. 2012, Acta Astronomica, 62, 281
Chatterjee, S., Cordes, J. M., Vlemmings, W. H. T., et al. 2004, ApJ, 604, 339
Cordes, J. M. & Lazio, T. J. W. 2002, ArXiv Astrophysics e-prints
Cruz-González, C., Recillas-Cruz, E., Costero, R., Peimbert, M., & Torres-Peimbert, S. 1974, Revista Mexicana de Astronomia y Astrofisica, 1, 211
Dias, W. S., Assafin, M., Flório, V., Alessi, B. S., & Líbero, V. 2006, A&A, 446, 949
Fűrész, G. 2008, PhD thesis, University of Szeged, Hungary
Francis, C. 2013, MNRAS, 436, 1343
Harding, P., Morrison, H. L., Olszewski, E. W., et al. 2001, AJ, 122, 1397
Hernquist, L. 1990, ApJ, 356, 359
Hobbs, G., Lyne, A. G., Kramer, M., Martin, C. E., & Jordan, C. 2004, MNRAS, 353, 1311
Høg, E., Fabricius, C., Makarov, V. V., & et al. 2000, A&A, 355, L27
Hoogerwerf, R., de Bruijne, J. H. J., & de Zeeuw, P. T. 2001, A&A, 365, 49
Hut, P. 1981, A&A, 99, 126
Kharchenko, N. V., Piskunov, A. E., Röser, S., Schilbach, E., & Scholz, R.-D. 2005, A&A, 440, 403
Lampens, P., Strigachev, A., & Duval, D. 2007, A&A, 464, 641
Lejeune, T. & Schaerer, D. 2001, A&A, 366, 538
Leonard, P. J. T. 1989, AJ, 98, 217
Manchester, R. N., Hobbs, G. B., Teoh, A., & Hobbs, M. 2005, AJ, 129, 1993
Mermilliod, J.-C. & Paunzen, E. 2003, A&A, 410, 511
Miyamoto, M. & Nagai, R. 1975, PASJ, 27, 533
Moffat, A. F. J., Marchenko, S. V., Seggewiss, W., & et al. 1998, A&A, 331, 949
Noutsos, A., Schnitzeler, D. H. F. M., Keane, E. F., Kramer, M., & Johnston, S. 2013, MNRAS, 430, 2281
Pietrinferni, A., Cassisi, S., Salaris, M., & Castelli, F. 2004, ApJ, 612, 168
Poveda, A., Ruiz, J., & Allen, C. 1967, Boletin de los Observatorios Tonantzintla y Tacubaya, 4, 86
Przybilla, N., Nieva, M. F., Heber, U., & Butler, K. 2008, ApJ, 684, L103
Schaerer, D., Meynet, G., Maeder, A., & Schaller, G. 1993, A&AS, 98, 523
Schaller, G., Schaerer, D., Meynet, G., & Maeder, A. 1992, A&AS, 96, 269
Schmidt-Kaler, T. H. 1982, Physical parameters of the stars, ed. K. Schaifers & H. H. Voigt
Smith, Jr., H. & Eichhorn, H. 1996, MNRAS, 281, 211
Stone, R. C. 1991, AJ, 102, 333
Tauris, T. M. & Takens, R. J. 1998, A&A, 330, 1047
Taylor, J. H. & Cordes, J. M. 1993, ApJ, 411, 674
Tetzlaff, N. 2013, PhD thesis, AIU, Friedrich-Schiller-Universität Jena, Germany
Tetzlaff, N., Dinçel, B., Neuhäuser, R., & Kovtyukh, V. V. 2014, MNRAS
Tetzlaff, N., Eisenbeiss, T., Neuhäuser, R., & Hohle, M. M. 2011a, MNRAS, 417, 617
Tetzlaff, N., Neuhäuser, R., & Hohle, M. M. 2009, MNRAS, 400, L99
Tetzlaff, N., Neuhäuser, R., & Hohle, M. M. 2011b, MNRAS, 410, 190
Tetzlaff, N., Neuhäuser, R., Hohle, M. M., & Maciejewski, G. 2010, MNRAS, 402, 2369
Tetzlaff, N., Schmidt, J. G., Hohle, M. M., & Neuhäuser, R. 2012, PASA, 29, 98
Tetzlaff, N., Torres, G., Neuhäuser, R., & Hohle, M. M. 2013, MNRAS, 435, 879
Torres, G., Neuhäuser, R., & Guenther, E. W. 2002, AJ, 123, 1701
van Leeuwen, F. 2007, A&A, 474, 653
Vande Putte, D., Garnier, T. P., Ferreras, I., Mignani, R. P., & Cropper, M. 2010, MNRAS, 407, 2109
Wu, Z.-Y., Zhou, X., Ma, J., & Du, C.-H. 2009, MNRAS, 399, 2146

© 2006 WILEY-VCH Verlag GmbH & Co. KGaA, Weinheim